IRK1 Inward Rectifier K$^+$ Channels Exhibit No Intrinsic Rectification

Donglin Guo and Zhe Lu

Department of Physiology, University of Pennsylvania, Philadelphia, PA 19104

ABSTRACT In intact cells the depolarization-induced outward IRK1 currents undergo profound relaxation so that the steady-state macroscopic I-V curve exhibits strong inward rectification. A modest degree of rectification persists after the membrane patches were perfused with artificial solutions devoid of Mg^{2+} and polyamines, which has been interpreted as a reflection of intrinsic channel gating and led to the view that inward rectification results from enhancement of the intrinsic gating by intracellular cations rather than simple pore block. Furthermore, IRK1 exhibits significant extracellular K$^+$-sensitive relaxation of its inward current, a feature that has been likened to the C-type inactivation observed in the voltage-activated *Shaker* K$^+$ channels. We found that both these current relaxations can be accounted for by impurities in some common constituents of recording solutions, such as residual hydroxyethylpiperazine in HEPES and ethylenediamine in EDTA. Therefore, inherently, IRK1 channels are essentially ohmic at the macroscopic level, and the voltage jump–induced current relaxations do not reflect IRK1 gating but the unusually high affinity of its pore for cations. Furthermore, our study helps define the optimal experimental conditions for studying IRK1.

KEY WORDS: EDTA • HEPES • hydroxyethylpiperazine • magnesium • polyamines

INTRODUCTION

Membrane depolarization–elicited outward current through inward rectifier K$^+$ channels exhibits profound relaxation. Consequently, with identical K$^+$ concentrations on both sides of the membrane the steady-state outward macroscopic current at positive membrane voltages is much smaller than the inward current at the corresponding negative voltages, a feature called initially anomalous rectification and subsequently inward rectification (Katz, 1949; Noble, 1965). The first clue to a possible mechanism came from the work by Armstrong and Binstock (1965), who showed that intracellular TEA blocks squid voltage–activated K$^+$ channels in a strongly voltage-dependent manner, rendering them inwardly rectifying. 20 y later, Mg^{2+} was identified as an endogenous voltage-dependent channel blocker causing inward rectification (Matsuda et al., 1987; Vandenberg, 1987). However, the voltage dependence of channel block by Mg^{2+} alone is too weak to account for the strong inward rectification observed in intact cells. Furthermore, significant rectification remains in the absence of Mg^{2+}. Thus arose the concept of intrinsic (voltage-dependent) channel gating to explain Mg^{2+}-independent current relaxation and rectification (e.g., Ishihara et al., 1989; Silver and DeCoursey, 1990; Stanfield et al., 1994).

Little progress was made in the search for additional endogenous blockers until certain polyamines were

found to block the channels in a strongly voltage-dependent manner (Ficker et al., 1994; Lopatin et al., 1994; Fakler et al., 1995). Still, variable residual inward rectification remains after the inside of a membrane patch is perfused with solutions nominally devoid of polyamines and Mg^{2+} (Aleksandrov et al., 1996; Shieh et al., 1996; Lee et al., 1999). This finding underlies the hypothesis that inward rectification results from intrinsic channel gating modulated by the binding of Mg^{2+} and polyamines to a putative channel-gating machinery, rather than from voltage-dependent channel block by these intracellular cations. We found, however, that the residual rectification independent of Mg^{2+} and polyamines is related to HEPES in recording solutions (Guo and Lu, 2000a).

Voltage jump–induced, time-dependent relaxation is not exclusively associated with outward currents, since hyperpolarization-induced inward currents also exhibit relaxation (Kubo et al., 1993). Choe et al. (1999) showed that hyperpolarization reduces the open probability of IRK1, and argued that the reduction in channel open probability results from both channel block by extracellular divalent cations and channel gating. Similar phenomena occur to a lesser extent in ROMK2 (Choe et al., 1998). Using IRK1-ROMK2 chimeras, Choe et al. (1999) found that the protein segments that form the ion conduction pore underlie the putative channel gating. Consistent with this, Lu et al. (2001) reported that gating of IRK1 at negative voltages is significantly perturbed when ester carbonyls replace the amide carbonyls of the two glycine residues within the signature sequence that forms the ion selectivity filter. Also, Shieh (2000) showed that in low K$^+$ solutions in

---

Address correspondence to Zhe Lu, Department of Physiology, D302A Richards Building, 3700 Hamilton Walk, University of Pennsylvania, Philadelphia, PA 19104. Fax: (215) 573-1940; E-mail: zhelu@mail.med.upenn.edu

FIGURE 1. Comparisons of the effects of intracellular HEPES, HEP, and piperazine on IRK1 currents (structures shown at top). (A–C) Currents were recorded with 10 mM HEPES, 3 μM HEP and 0.3 μM piperazine, respectively, from the same inside-out patch with the voltage pulse protocol shown below. In all cases the intracellular solutions contained 100 mM K$^+$, 5 mM EDTA, and 10 mM phosphate (pH 7.6) besides the tested chemicals, whereas the extracellular solution contained 100 mM K$^+$, 0.3 mM Ca^{2+}, 1 mM Mg^{2+}, 10 mM phosphate (pH 7.6). The currents are corrected for background current. Dotted lines identify the zero current level. (D–F) Normalized I-V curves, corresponding to A–C, which were constructed from the currents determined at the end of each test voltage-pulse. Current at each voltage is normalized (except for its signs) to that at −100 mV. Each data point represents the mean (± SEM) of currents recorded from 5–7 patches.
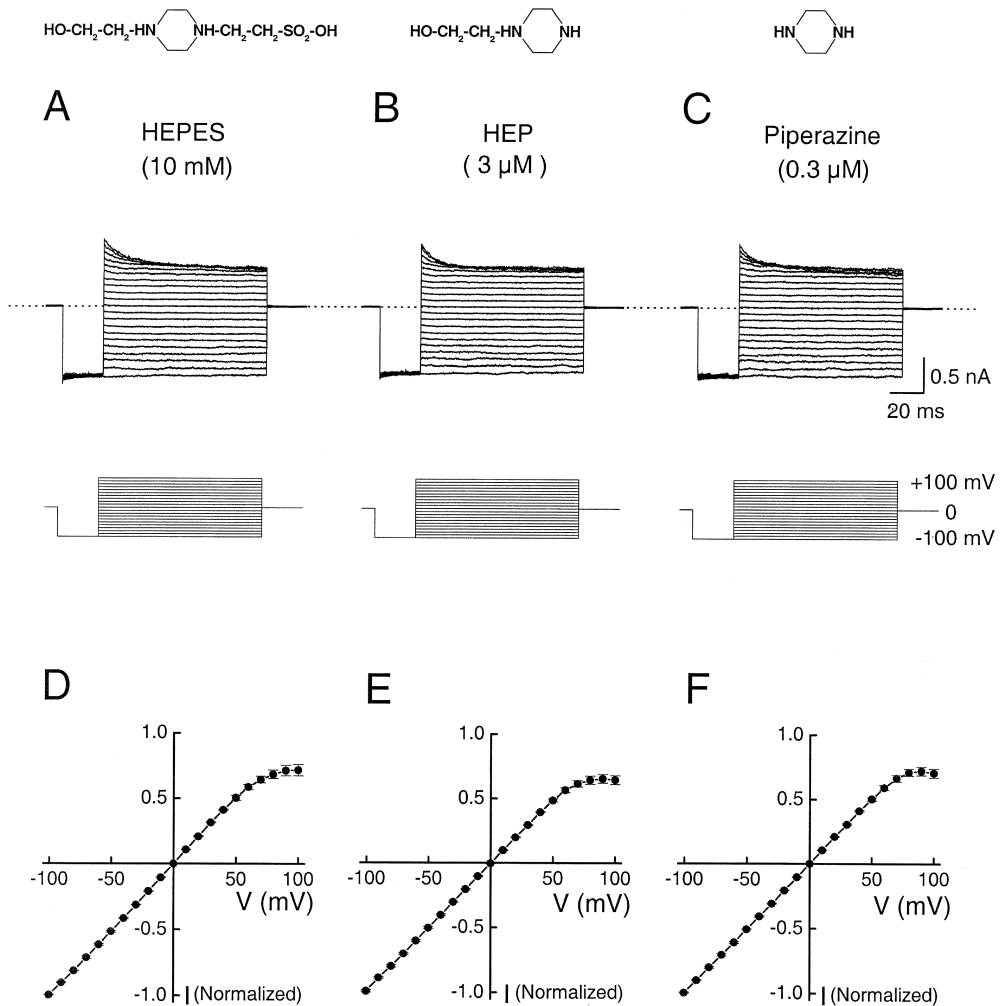
the absence of extracellular divalent cations, hyperpolarization induces a significant inward current relaxation which is likened to the C-type inactivation of voltage-activated *Shaker* K$^+$ channels (Hoshi et al., 1991; Lopez-Barneo et al., 1993; Yellen et al., 1994).

To resolve the fundamental issue whether the macroscopic conductance of IRK1 has any significant intrinsic voltage dependence, we present here a systematic experimental investigation of the causes underlying voltage jump–induced current relaxations. Our study also helps define the optimal experimental conditions for studying IRK1.

MATERIALS AND METHODS

Molecular Biology and Oocyte Preparation

IRK1 cDNA (Kubo et al., 1993) was cloned into the pGEM-Hess plasmid. RNA was synthesized using T7 polymerase (Promega) from Nhe1-linearized cDNAs. Oocytes harvested from *Xenopus laevis* (*Xenopus* One) were incubated in a solution containing NaCl, 82.5 mM; KCl, 2.5 mM; MgCl$_2$, 1.0 mM; HEPES (pH 7.6), 5.0 mM; and collagenase, 2–4 mg/ml. The oocyte preparation was agitated at 80 rpm for 60–90 min. It was then rinsed thor-

oughly and stored in a solution containing NaCl, 96 mM; KCl, 2.5 mM; CaCl$_2$, 1.8 mM; MgCl$_2$, 1.0 mM; HEPES (pH 7.6), 5 mM; and gentamicin, 50 μg/ml. Defolliculated oocytes were selected and injected with RNA at least 2 and 16 h, respectively, after collagenase treatment. All oocytes were stored at 18°C.

Patch Recording

IRK1 currents were recorded from inside-out membrane patches of *Xenopus* oocytes (injected with IRK1 cRNA) with an Axopatch 200B amplifier (Axon Instruments, Inc.), filtered at 5 kHz, and sampled at 25 kHz using an analogue-to-digital converter (DigiData 1200; Axon Instruments, Inc.) interfaced with a personal computer. pClamp6 software (Axon Instruments, Inc.) was used to control the amplifier and acquire the data. During current recording, the voltage across the membrane patch was first hyperpolarized from the 0 mV holding potential to −100 mV and then stepped to various test voltages, or stepped directly from the holding potential. The duration of the voltage test pulse was 100 ms, which is comparable to those used in the studies where the Mg^{2+}- and polyamine-independent rectification was initially observed (Aleksandrov et al., 1996; Shieh et al., 1996). Background leak current correction was performed as described previously (Lu and MacKinnon, 1994; Guo and Lu, 2000a). To effectively perfuse the patch, the tip of the patch pipette (∼3 MΩ) was immersed in a stream of intracellular solution exiting one of ten glass capillaries (ID = 0.2 mm) mounted in parallel.
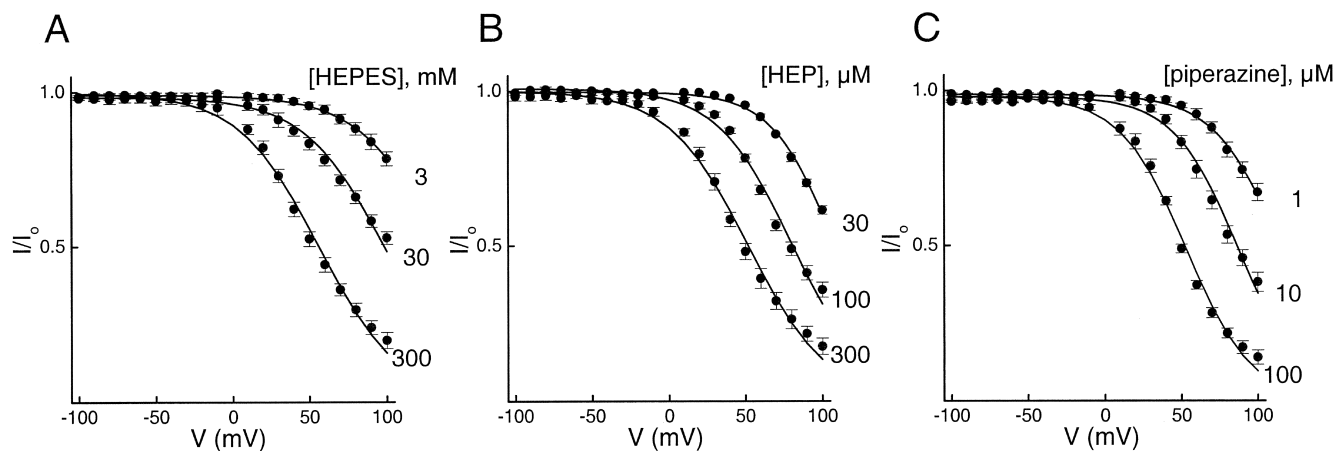
FIGURE 2. HEPES, HEP, and piperazine concentration dependence of channel block. The fraction of unblocked currents in the presence of three representative concentrations of HEPES (A), HEP (B), or piperazine (C) is plotted against membrane voltage. The theoretical curves are fits of the Woodhull equation, which give $K_d(0 \text{ mV}) = 2.47 \pm 0.02$ M (mean $\pm$ SEM, $n = 6$) and $Z = 1.02 \pm 0.02$ for HEPES, $K_d(0 \text{ mV}) = 2.97 \pm 0.16$ mM ($n = 6$) and $Z = 1.09 \pm 0.03$ for HEP, and $K_d(0 \text{ mV}) = 0.27 \pm 0.04$ mM ($n = 8$) and $Z = 1.08 \pm 0.02$ for piperazine.

Recording Solutions

All recording solutions contained 100 mM K^+ contributed by KCl, K_2EDTA, K_2HPO$_4$, KH$_2$PO$_4$, and KOH. The phosphate-buffered intracellular solution contained (mM): 5 K_2EDTA (unless specified otherwise), 10 "K_2HPO$_4$ + KH$_2$PO$_4$" in a ratio yielding the desired pH, and sufficient KCl to bring total K^+ concentration to 100 mM (Guo and Lu, 2000a). To adjust pH to 8.0 and above a small amount of KOH was used. The HEPES-buffered intracellular solution, used in Fig. 3, contained (mM): 100 K^+ (Cl$^-$ + OH$^-$), 5 EGTA and 10 HEPES, pH 7.2 (adjusted with KOH). The HEPES-buffered extracellular solution contained (mM): 100 K^+ (Cl$^-$ + OH$^-$), 0.3 CaCl$_2$, 1.0 MgCl$_2$, and 10 HEPES, pH 7.6 (adjusted with KOH). In the phosphate-buffered extracellular solution, HEPES was replaced by an equal concentration of "K_2HPO$_4$ + KH$_2$PO$_4$" in a ratio yielding pH 7.6. The divalent cation-free extracellular solution contained 5 mM EDTA. All chemicals were purchased from Fluka Chemical Corp.

RESULTS

We showed previously that intracellular "HEPES" blocks IRK1 channels with varying potency depending on the commercial sources (Guo and Lu, 2000a). As shown there and in Fig. 1 A, the blocking kinetics are slow even with 10 mM HEPES present. These findings indicate that the block is caused mainly by some impurity in HEPES. Usually, HEPES is synthesized by reacting hydroxyethylpiperazine (HEP)* with bromoethanesulfonate (Good et al., 1966). Fig. 1 B shows the current records in the presence of 3 μM HEP; the I-V curves determined at the end of the voltage pulses in the presence of 10 mM HEPES and 3 μM HEP are shown in
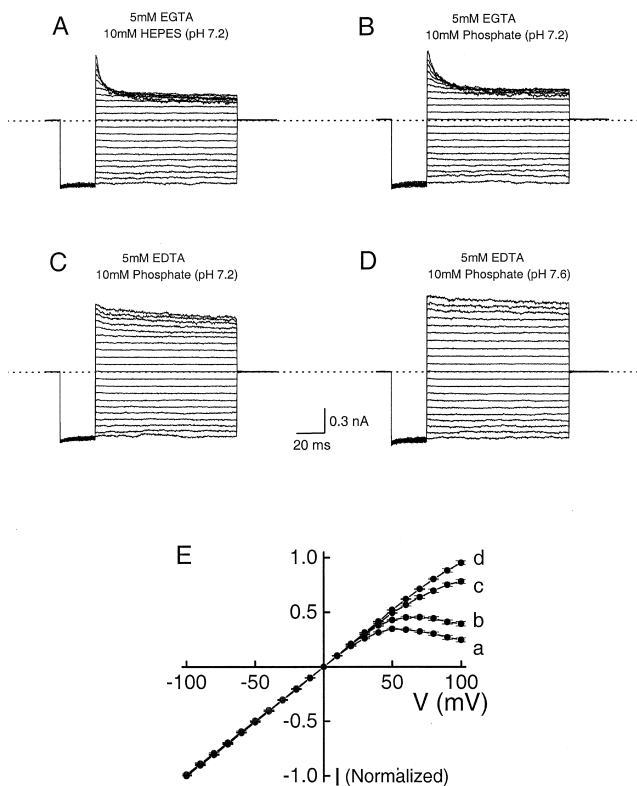

FIGURE 3. Other causes underlying apparent inward rectification. (A–D) Currents were recorded from the same inside-out patch with the voltage pulse protocol shown in Fig. 1. The intracellular solution composition (besides KCl) and pH for each panel are indicated. (E) Normalized I-V curves constructed from the currents determined at the end of each test voltage-pulse. The I-V curves a–d correspond to the currents from A–D, respectively. All data points are mean $\pm$ SEM ($n = 5$).

Abbreviations used in this paper: HEP, hydroxyethylpiperazine; ppm, part per million.

A

5 mM EDTA   5 mM CDTA   5 mM EGTA

|1 nA
20 ms

B

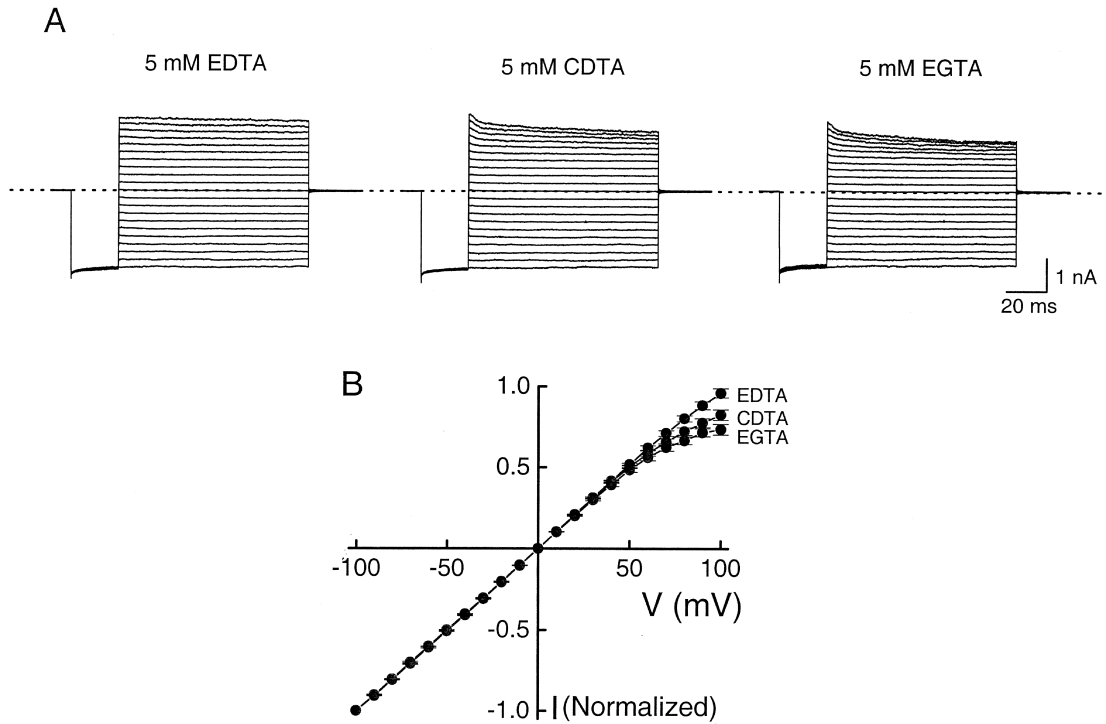

EDTA
CDTA
EGTA

V (mV)

I (Normalized)

FIGURE 4.   IRK1 currents in the presence of three metal ion chelators. (A) Current records collected from the same patch in the presence of intracellular EDTA, EGTA, or CDTA, each at 5 mM. Phosphate was used to buffer pH. (B) Normalized I-V curves in the presence of the metal ion chelators. All data points are mean $\pm$ SEM ($n = 5$).

Fig. 1, D and E, respectively. HEPES and HEP block the channels in a qualitatively comparable manner, although HEP is much more potent. The blocking activity of HEP must come from the piperazine ring since piperazine itself is even more potent (Fig. 1, B versus C,

and E versus F). Fig. 2 shows the fraction of unblocked currents in the presence of three representative concentrations of HEPES, HEP, or piperazine. Analyzing the data in Fig. 2 with the Woodhull (1973) equation gives an apparent K_d(0 mV) = 2.47 M and Z (va-

0.1 mM EDTA   1 mM EDTA

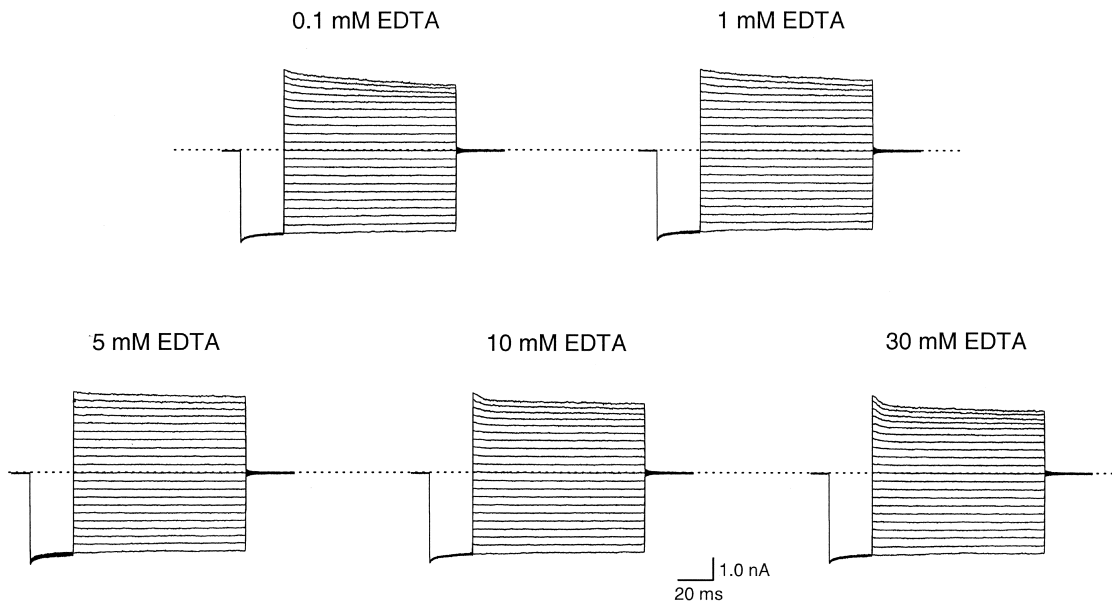5 mM EDTA   10 mM EDTA   30 mM EDTA

|1.0 nA
20 ms

FIGURE 5.   Effects of EDTA concentration on IRK1 currents. All traces were recorded from the same patch, with intracellular EDTA concentrations as indicated. The corresponding I-V curves are shown in Fig. 6. Solution pH was buffered with phosphate.
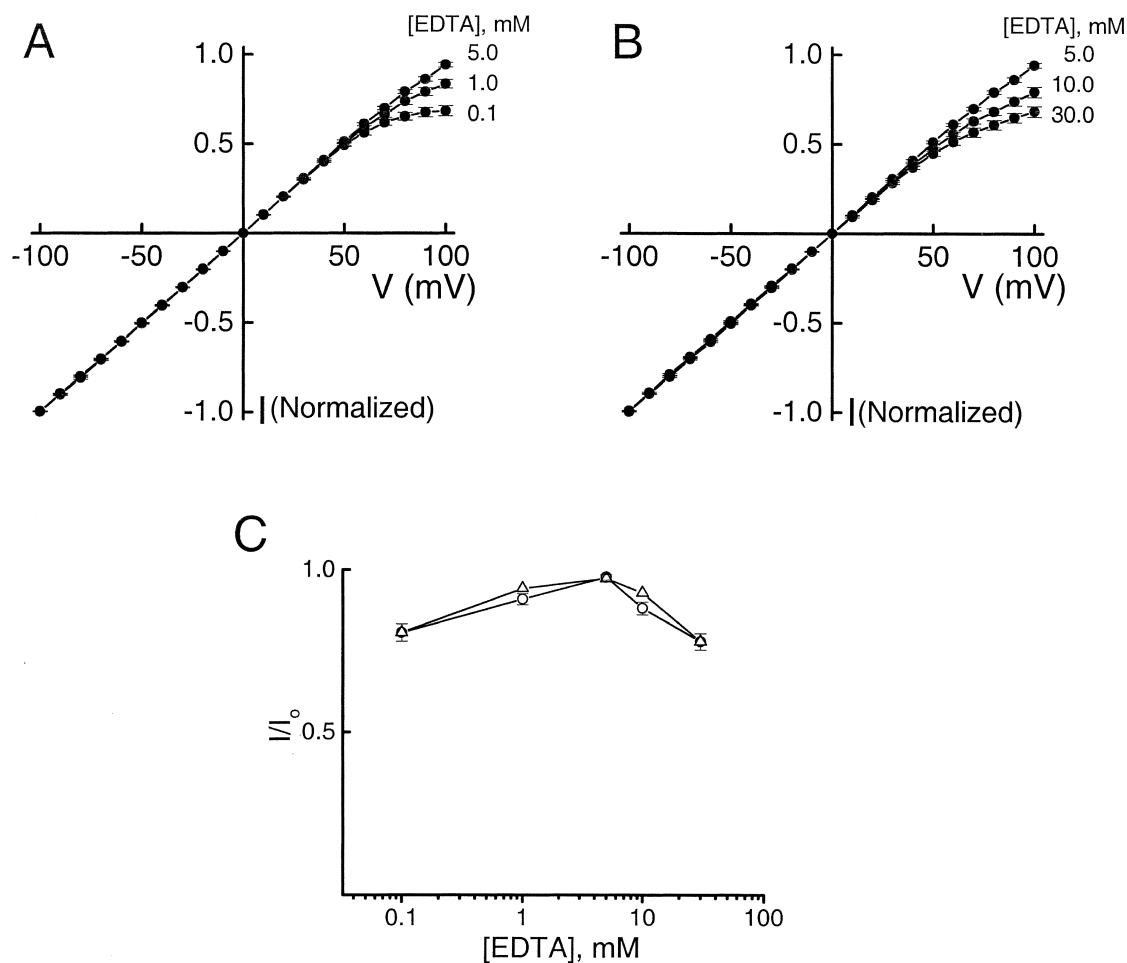
FIGURE 6. Effects of EDTA concentration on the I-V curves of IRK1 channels. Normalized I-V curves in the presence of various concentrations of EDTA. For clarity, I-V curves with 0.1–5 mM intracellular EDTA (A) are plotted separately from those with 5–30 mM EDTA (B). All data points are mean ± SEM (n = 4–6). (C) Normalized current at 80 mV, taken from the I-V curves in A and B, is plotted against the concentration of EDTA. The data represented by the circles (mean ± SEM) were determined experimentally, whereas those by triangles were calculated using Eq. 1, as described in DISCUSSION.

lence) = 1.02 for HEPES, K_d(0 mV) = 2.97 mM and Z = 1.09 for HEP, and K_d(0 mV) = 0.27 mM and Z = 1.08 for piperazine. Therefore, the apparent channel block by HEPES can be accounted for by a trace amount of HEP, which is well below the limit of impurity specified by the supplier (0.5%).

To our surprise, we found in the experiment shown below that HEPES is not the sole source of contaminating blockers in commonly used intracellular solutions. Fig. 3 shows that IRK1 channels exhibit inward rectification in the presence of an intracellular solution like that used by Aleksandrov et al. (1996), which contained KCl, EGTA and HEPES (pH 7.2). The rectification was reduced only modestly when HEPES (10 mM) was replaced by phosphate (10 mM), but reduce significantly further when we also substituted EDTA (5 mM) for EGTA (5 mM), although the I-V curve did not approach linearity until solution pH was raised from 7.2 to 7.6 [the final composition is the one we used previ-

ously (Guo and Lu, 2000a)]. These findings show that the persisting rectification after removal of endogenous blockers (Aleksandrov et al., 1996) was caused by the use of HEPES, EGTA, and low pH. Intracellular EGTA, HEPES (each up to 10 mM), and pH < 7.4 have been widely used in studies of IRK1.

Fig. 4 compares the effects of intracellular metal ion chelators EDTA, CDTA, or EGTA (each at 5 mM; pH 7.6) on the currents and the I-V curves. Inward rectification is more pronounced with either EGTA or CDTA than with EDTA, even though the affinity of CDTA for a given di- or trivalent cation is much higher than that of EDTA. Since EDTA causes the least rectification and also is nonselective among divalent cations, EDTA instead of EGTA should be used to scavenge contaminating blocking metal ions. To find the intracellular EDTA concentration that yields the most linear I-V curve (at pH 7.6, see below), we obtained current records from the same patch in the presence of five different concen-
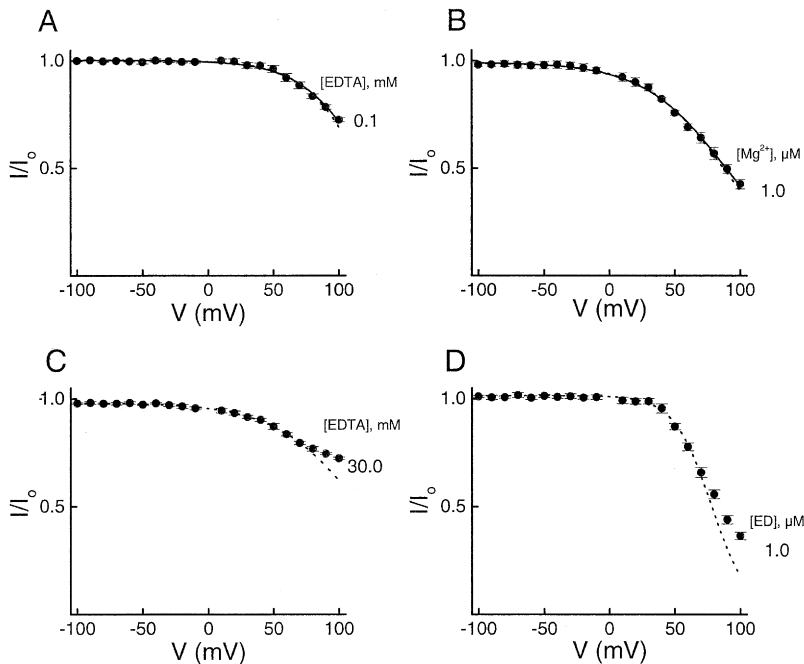
FIGURE 7. Comparisons of channel block by "EDTA" with block by Mg^{2+} or ethylenediamine. (A and C) Currents with 0.1 mM and 30 mM EDTA normalized to that with 5 mM EDTA are plotted against membrane voltage, respectively. (B and D) The fraction of unblocked currents in the presence of Mg^{2+} or ethylenediamine (ED), respectively, is plotted against membrane voltage. All data points are mean $\pm$ SEM ($n = 5$). All curves are fits of the equation $I/I_o = 1/(1 + [blocker]/K_d)$, where $K_d = K_d(0\ mV)e^{-ZFV/RT}$. For A and B, the two nearly superimposed curves for each data set are fits either all data points (continuous curves) or all but the rightmost three data points (dashed curves). For C or D, the dashed curve through each dataset is a fit to all but the rightmost three data points.

trations of EDTA (Fig. 5). With 0.1 mM EDTA, outward currents displayed modest inward rectification. As the chelator concentration was raised to 5 mM the rectification is nearly vanished, most probably because the concentration of contaminating free blocking metal ions was reduced. However, when EDTA concentration was increased further, rectification became again more pronounced, presumably reflecting the effect of some impurity in EDTA. For clarity, I-V curves for 0.1–5 mM and for 5–30 mM EDTA are plotted separately in Fig. 6 A, and B, showing that 5 mM EDTA is optimal for obtaining a linear macroscopic I-V curve. The normalized current (mean $\pm$ SEM) at 80 mV, taken from the I-V curves in A and B, is plotted against the concentration of EDTA (Fig. 6 C, circles).

Fig. 7 plots the fraction of unblocked currents in the presence of a low (0.1 mM; Fig. 7 A) or a high (30 mM; Fig. 7 C) concentration of EDTA against membrane voltage. The two blocking curves differ in character. At 0.1 mM EDTA, it is well described by the Woodhull (1973) equation (Fig. 7 A), consistent with that the channels were blocked by a "nonpermeant" blocker such as a divalent cation, an example of which (block by Mg^{2+}) is shown in Fig. 7 B. In contrast, at 30 mM EDTA the blocking curve deviates from the Woodhull equation (Fig. 7 C), consistent with that the channels were blocked by a permeant blocker such as ethylenediamine (ED, Fig. 7 D; see Guo and Lu, 2000b for details). Fig. 8, A and B, shows the current records with 30 mM EDTA and 0.1 μM ethylenediamine, respectively; the corresponding I-V curves are shown in Fig. 8, C and D. EDTA and ethylenediamine block the channels in a qualitatively comparable manner, although the latter is

>10,000-fold more potent. Therefore, the blocking effect associated with EDTA can be accounted for by trace of contaminating ethylenediamine used to synthesize EDTA. All subsequent data were recorded with intracellular solutions containing 5 mM EDTA and 10 mM phosphate (without HEPES).

To determine the optimal intracellular pH we examined how pH affects IRK1 currents (Fig. 9 A). The average I-V curve for each pH examined is plotted in Fig. 10 A. The I-V curve is linear at pH 8.5. Lowering pH inhibited IRK1 currents minimally between 8.5 and 7.5 but dramatically between 7.5 and 6.5. The fraction of current not inhibited by protons is plotted in Fig. 10 C, which shows that channel inhibition has voltage-dependent and -independent components. Interestingly, much of the voltage-dependent component of proton inhibition vanished when acidic D172 (located in the inner pore) was replaced by neutral asparagine (Figs. 9 B, and 10, B and D). At higher intracellular pH the outward D172N current is slightly larger than the inward current.

As a practical matter, very small membrane patches must be used to achieve adequate removal of endogenous blockers by perfusion. To illustrate this, Fig. 11 A shows three consecutive sets of current records from a small membrane patch, taken at 1-min intervals after the start of perfusion. Any endogenous blockers present in that excised patch were apparently effectively removed within the first minute. In contrast, for a much larger patch (from a separate oocyte injected with much less RNA), removal of endogenous blockers was very slow and incomplete even after prolonged perfusion (Fig. 11 B).
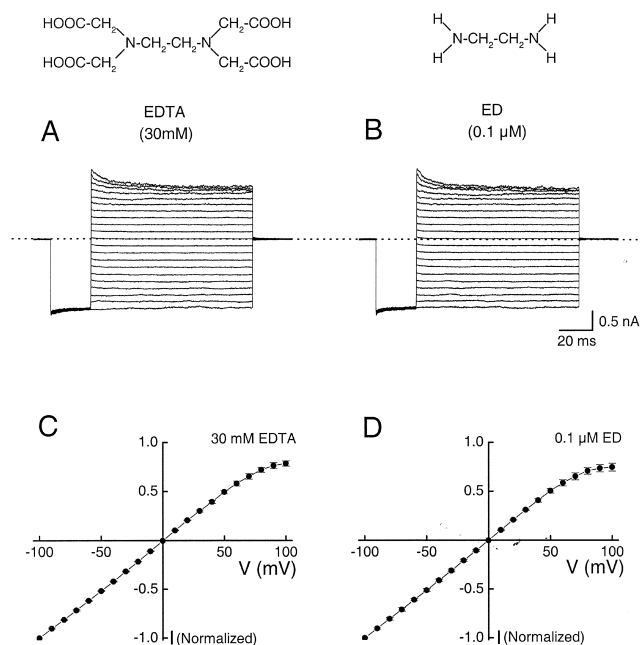
FIGURE 8. Comparisons of the effects on IRK1 currents of intracellular EDTA and ethylenediamine (structures shown at top). (A and B) Currents were recorded from the same membrane patch with, respectively, 30 mM EDTA and 0.1 μM ethylenediamine. (C and D) Normalized I-V curves; each data point represents the mean (± SEM; $n = 5$) of currents.
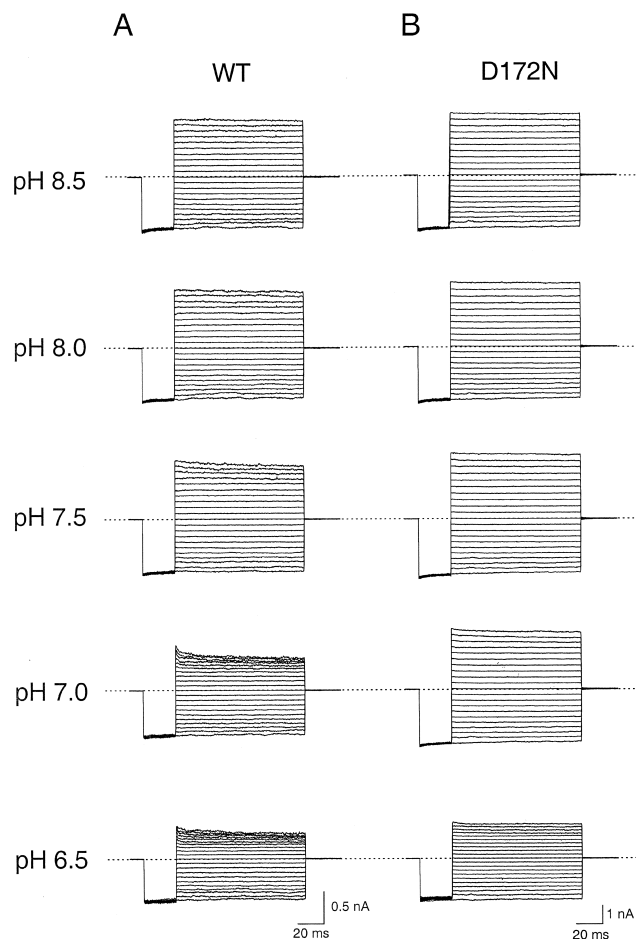

FIGURE 9. Effects of intracellular pH on the currents of wild-type and D172N mutant IRK1 channels. Currents were recorded at various intracellular pH, with extracellular pH = 7.6 throughout. For each channel type, all currents were obtained from the same inside-out patch.

Under certain commonly used experimental conditions membrane hyperpolarization also induces relaxation of inward IRK1 currents. The currents in Fig. 12 A (and all those above) were recorded with 0.3 mM Ca^{2+} and 1.0 mM Mg^{2+} present in the extracellular solution buffered with phosphate. The inward currents at very negative voltages relax noticeably. This relaxation largely vanished (Fig. 12 B) in the absence of extracellular divalent cations. The voltage dependence of the ratio of currents at the end and the beginning of voltage pulses (I_{end}/I_{bgn}) is shown in Fig. 12 C. These results are consistent with the previous finding by Choe et al. (1999) that extracellular divalent cations block IRK1 in a voltage-dependent manner.

Furthermore, Shieh (2000) observed relaxation of inward current even in the nominal absence of extracellular divalent cations. The relaxation was prominent only at low concentrations of K^+. Since solutions in the quoted study were HEPES buffered, we wondered whether the current relaxation was due to the use of extracellular HEPES. Confirming the results of Shieh (2000), we found that the inward current after strong membrane hyperpolarization exhibits little or no relaxation when the extracellular solution contained 100 mM K^+, 10 mM HEPES, and 5 mM EDTA, but no added divalent cations (Fig. 13 A). Replacing HEPES with phosphate had no noticeable effect (Fig. 13 C).

Also confirming Shieh's finding, lowering the K^+ concentration to 20 mM revealed prominent inward current relaxation (Fig. 13 B). However, this relaxation vanished when we replaced HEPES with phosphate (Fig. 13 D). The voltage dependence of the ratio of currents at the end and the beginning of voltage pulses (I_{end}/I_{bgn}) is shown in Fig. 13 E. Furthermore, we examined whether channel block associated with extracellular HEPES could also be caused by residual contaminants. As shown in Fig. 14, like "HEPES", HEP and piperazine block the channels in the presence of 20 mM but not 100 mM extracellular K^+. Therefore, channel block associated with extracellular HEPES can also be accounted for by a trace amount of contaminating HEP.

DISCUSSION

In the present study, we systematically investigated the causes underlying the reported IRK1 current relax-
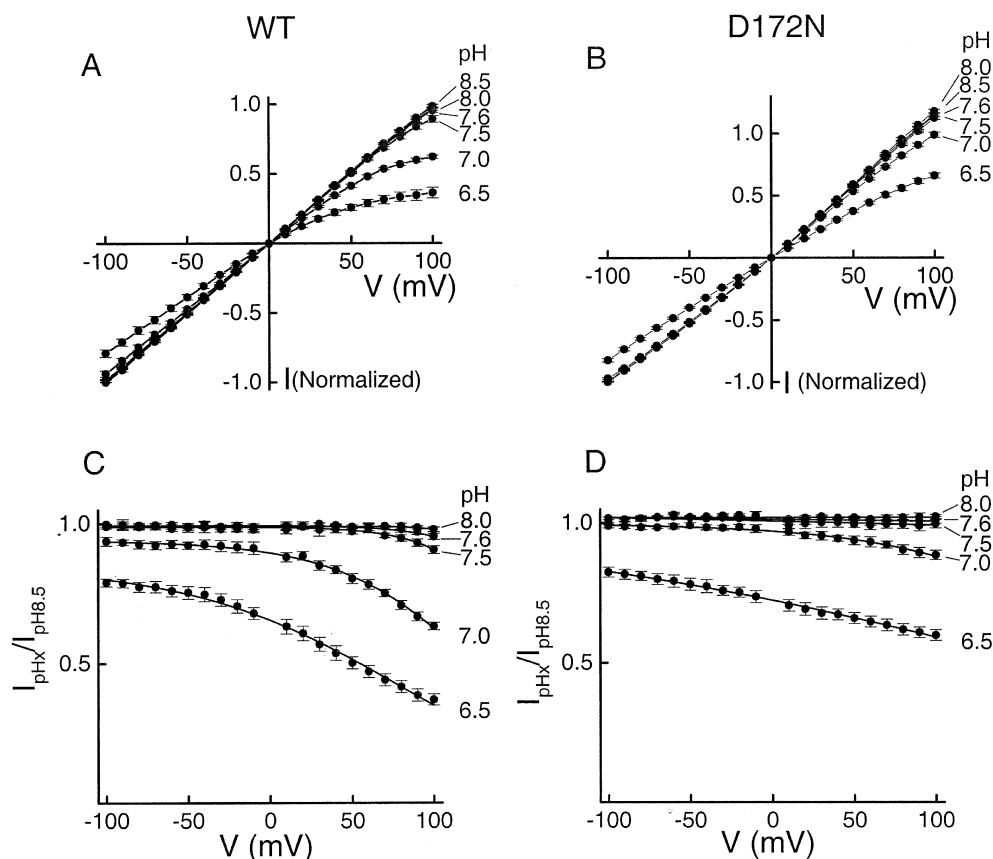
FIGURE 10. Effects of intracellular pH on the I-V curves of wild-type and mutant IRK1 channels. (A and B) I-V curves of wild-type and D172N mutant IRK1 channels at various intracellular pH, determined from the current records, as shown (and including those) in Fig. 9, except for those at pH 7.6, which were taken from those as shown in Fig. 4 A. (C and D) Currents through IRK1 and D172N channels, normalized to those at pH 8.5, are plotted against membrane voltage. All data points are mean ± SEM ($n = 5$).

ations after step changes of membrane voltage, and found that none of them is intrinsic to the channels. In other words, within the usual voltage range the macroscopic IRK1 conductance has no significant intrinsic voltage dependence that causes either inward rectification or inactivation. The reported apparent voltage dependence of macroscopic IRK1 currents is caused by traces of contaminants in routinely used chemicals, such as HEPES and metal ion chelators among which (the latter) EDTA has the least effect. Specifically, block associated with both intracellular and extracellular HEPES can be accounted for by residual HEP (~500 part per million (ppm) in weight), and that associated with intracellular EDTA by residual ethylenediamine (~1 ppm). These contamination levels, estimated from the relative specific inhibitory activity of compared chemicals (Figs. 2 and 8), are well below the limits (5,000 ppm) specified by the supplier.

Intracellular divalent chelators must be used both to suppress endogenous Ca^{2+}-activated Cl^- currents and to minimize channel block by contaminating divalent cations. However, a divalent cation chelator such as EDTA has two opposing effects: (a) it reduces free divalent cation concentration and thereby relieves channel block by these ions, and (b) it contains residual ethylenediamine that blocks the channels. Consequently, the current is a biphasic function of EDTA concentra-

tion with a maximum at an intermediate concentration of EDTA (Fig. 6), which may vary somewhat depending on the extent of contamination in a given lot of EDTA and on the level of divalent cation concentration in the solution. Under the present solution conditions, the maximal current corresponding to 5 mM EDTA where there is little time-dependent relaxation of outward current during a 100-ms test-pulse to positive voltage (even up to 100 mV; Fig. 5), which is sufficiently long for many common studies.

In the solution with 0.1 mM EDTA the estimated concentration of contaminating ethylenediamine is ~0.3 nM (Fig. 8), which practically causes no channel block, given that the $^{ED}K_d(0 \text{ mV}) = 1.4$ mM and $^{ED}Z = 2$ (Guo and Lu, 2000b). Therefore, at this low concentration of EDTA the channels are blocked primarily by contaminating metal ions (Fig. 7). The common divalent cations, Ca^{2+} and Mg^{2+}, block inward rectifiers with the same mechanism, although the latter binds with somewhat higher affinity (Matsuda, 1993; Matsuda and Cruz, 1993). Examining block by intracellular Ca^{2+} is technically more difficult due to the presence of Ca^{2+}-activated Cl^- currents in oocytes; thus, we estimated the total concentration of contaminating divalent cations in the equivalent of Mg^{2+}. To do so, we first determined that $^{Mg}K_d$ (0 mV) = 17 μM and $^{Mg}Z = 1.1$ from the fit of the Woodhull equation to the Mg^{2+}-inhibition curve (Fig. 7

A

1 min   2 min   3 min

0.5 nA
20 ms

B

1 min   2 min   3 min

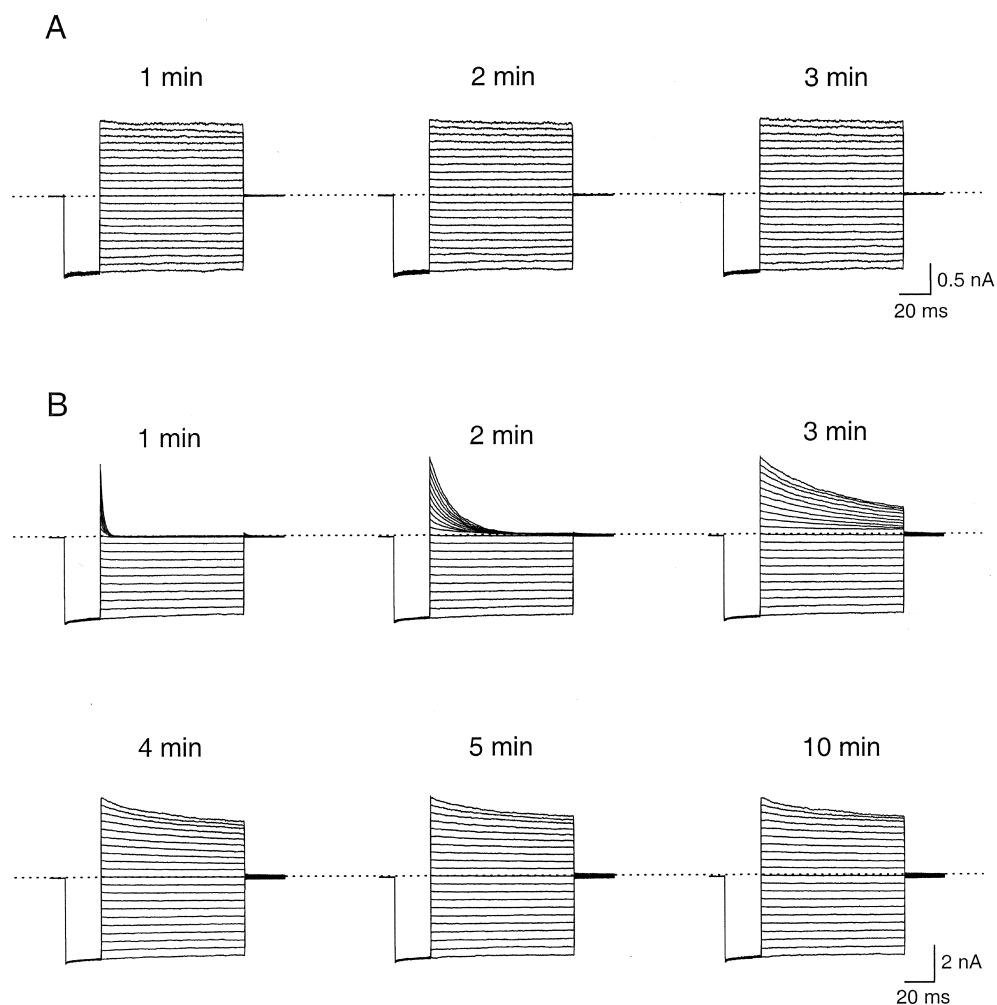4 min   5 min   10 min

2 nA
20 ms

FIGURE 11. Variable degree and rate of removal of endogenous blockers by perfusion. Current traces shown in A and B were recorded from two separate patches excised from two oocytes injected with different amounts of cRNA (higher in A than in B). The recordings were made at the indicated times following the start of perfusion.

B). Then, based on these values, we found, from the same analysis of current inhibition in 0.1 mM EDTA, that the extent of channel block is equivalent to that caused by 68 nM free Mg^{2+} (Fig. 7 A). This free Mg^{2+} concentration requires 20 μM total Mg^{2+} in a 0.1 mM EDTA solution while the EDTA-Mg^{2+} stability constant is 3.5×10^6 M^{-1}. Theoretically, 20 μM Mg^{2+} in a 30 mM EDTA solution results in 0.2 nM free Mg^{2+}, which would practically cause no block. Thus, at this high EDTA concentration the channels are primarily blocked by contaminating ethylenediamine (0.1 μM; Fig. 8). With these estimates, we calculated for each EDTA concentration the current at 80 mV, using the following equation,

$$\frac{I}{I_O} = \frac{1}{1 + \dfrac{[Mg^{2+}]_{free}}{{}^{Mg}K_d(0\ mV)e^{-\frac{{}^{Mg}ZFV}{RT}}} + \dfrac{[ED]}{{}^{ED}K_d(0\ mV)e^{-\frac{{}^{ED}ZFV}{RT}}}}, \quad (1)$$

where quantities F, V, R, and T have their usual meaning. Since the current at 80 mV does not significantly deviate from the fit of the Woodhull equation (Fig. 7, C

and D), ethylenediamine is assumed, for simplicity, to be nonpermeant. The calculated values with the equation agree well with those experimentally observed (Fig. 6 C).

As in the case of other inward rectifiers, lowering intracellular pH significantly inhibits IRK1 (Shieh et al., 1996). Fig. 10, A and C, shows that inhibition by protons has both voltage-dependent and -independent components. Several residues underlying voltage-independent inhibition by intracellular protons have been identified in various inward rectifiers (e.g., Fakler et al., 1996; Xu et al., 2000). On one hand, if D172 in the pore of IRK1 acts as a surface charge and if protonation of D172 is voltage dependent, protonation of D172 (D^- to D) may reduce the single channel conductance and thereby render the channels inwardly rectifying. For the following reasons, this may not, however, be the primary cause underlying the observed voltage-dependent channel inhibition at low pH. Replacing D172 with neutral asparagine does not reduce the single channel conductance (Oishi et al., 1998). Furthermore, it renders neither the single channel i-V curve
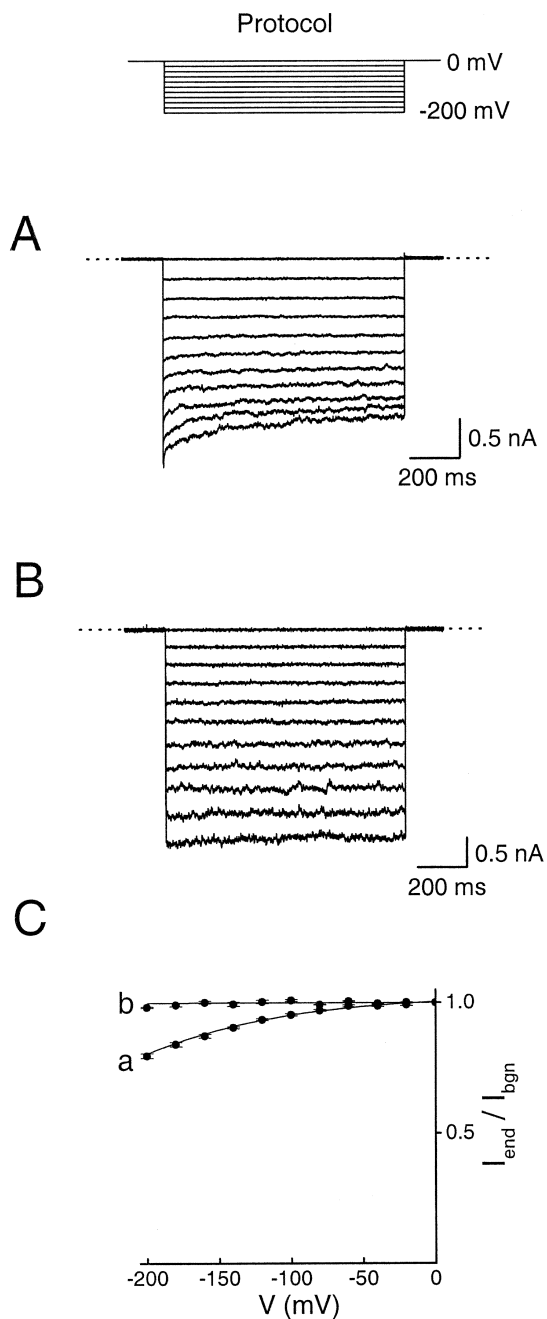
Protocol

A

B

C

FIGURE 12. Relaxation of inward currents caused by extracellular divalent cations. Currents were recorded with the voltage protocol shown at the top. Intra- and extracellular solutions were buffered with 10 mM phosphate. The extracellular solution contained 0.3 mM Ca^{2+} and 1 mM Mg^{2+} in A, but 5 mM EDTA and no added Ca^{2+} or Mg^{2+} in B. (C) The ratio of currents at the end and the beginning of voltage pulses (I_{end}/I_{bgn}) is plotted against membrane voltage. The data corresponding to A and B are labeled by letters a and b, respectively. All data points are mean $\pm$ SEM ($n = 5$).

nor the macroscopic I-V curve inwardly rectifying (Oishi et al., 1998; Guo and Lu, 2000a; Fig. 10 B). On the other hand, voltage-dependent inhibition of IRK1 by intracellular protons probably primarily reflects pro-
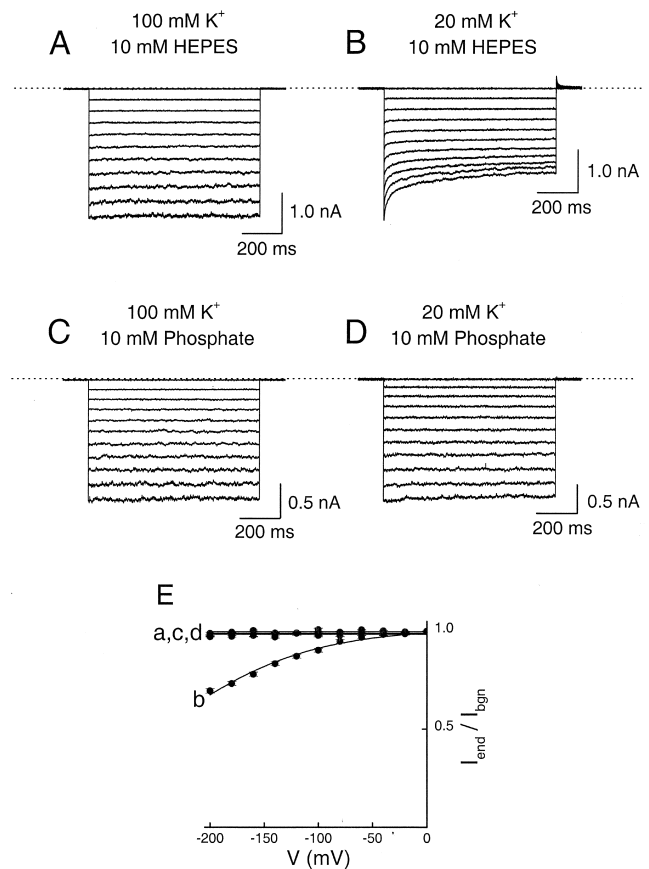
A 100 mM K⁺ 10 mM HEPES B 20 mM K⁺ 10 mM HEPES

C 100 mM K⁺ 10 mM Phosphate D 20 mM K⁺ 10 mM Phosphate

E

FIGURE 13. K^+ dependence of the inward current relaxation in the presence of extracellular HEPES. All currents were elicited with the voltage protocol shown in Fig. 12, with 5 mM EDTA and no added divalent cations present in the extracellular solution. Extracellular solutions were buffered with 10 mM HEPES (A and B) or phosphate (C and D), and contained either 100 mM K^+ (A and C) or 20 mM K^+ (B and D). (E) The ratio of currents at the end and the beginning of voltage pulses (I_{end}/I_{bgn}) is plotted against membrane voltage. The data corresponding to A–D are labeled a–d, respectively. All data points are mean $\pm$ SEM ($n = 5$).

tonation of amine groups in the residual endogenous and contaminating exogenous organic blockers and/ or EDTA. Protonation of these blockers enhances their affinity for IRK1 (Guo and Lu, 2000b), whereas protonation of EDTA reduces its affinity for trace divalent cations, thus causing further channel block. Consistent with this reasoning, mutant D172N channels, whose affinity for intracellular blocking cations is dramatically reduced (Lopatin et al., 1994; Ficker et al., 1994; Fakler et al., 1995; Yang et al., 1995), exhibit dramatically reduced voltage-dependent inhibition at low pH (Fig. 10 D). In any case, for practical purposes one can obtain essentially uninhibited IRK1 currents at intracellular pH 7.6 or higher.

The affinity of IRK1 channels for some endogenous blockers is exceedingly high, so that even trace amounts of endogenous blocker may cause significant
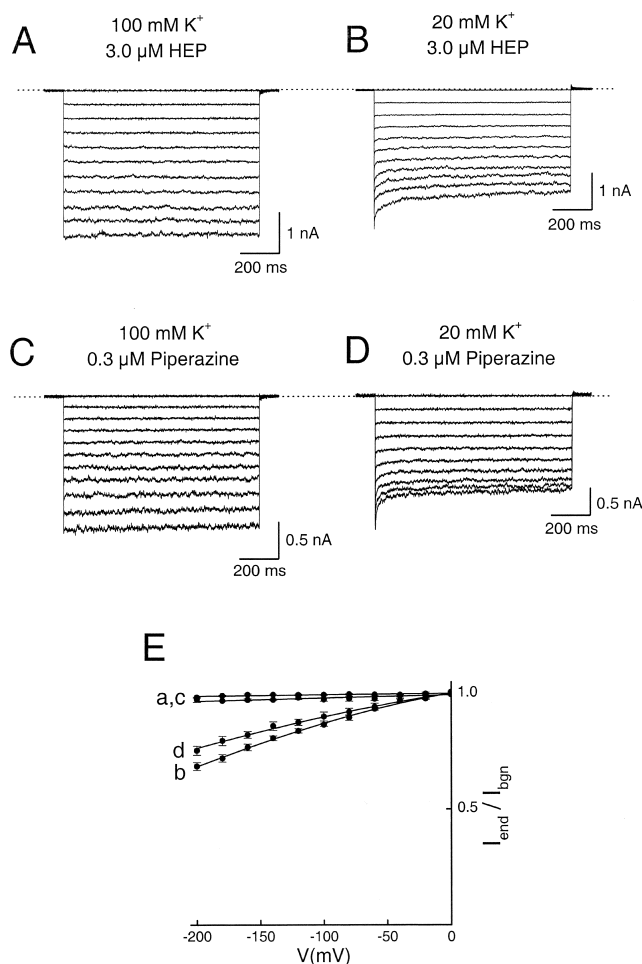
FIGURE 14. K$^+$ dependence of inward current relaxation in the presence of extracellular HEP or piperazine. Intra- and extracellular solutions were buffered with 10 mM phosphate. The extracellular solution contained 3 μM HEP (A and B) or 0.3 μM piperazine (C and D), and either 100 mM K$^+$ (A and C) or 20 mM K$^+$ (B and D). (E) The ratio of currents at the end and the beginning of voltage pulses (I_{end}/I_{bgn}) is plotted against membrane voltage. The data corresponding to A–D are labeled a–d, respectively. All data points are mean ± SEM ($n = 5$).

inward rectification. For example, the K$_d$(0 mV) for the binding of fully protonated spermine is ~10^{-7} M, whereas the effective valence of channel block by spermine is ~5 (Guo and Lu, 2000a,b). The calculated K$_d$(100 mV) for spermine binding is therefore ~10^{-15} M, which is almost certainly below the concentration of spermine remaining in an exhaustively perfused membrane patch. Therefore, although spermine is a permeant blocker whose effect can be somewhat relieved by membrane depolarization, at 100 mV in the steady-state most channels will be blocked by spermine at concentrations as low as 1 nM (typical oocyte concentrations are submillimolar; Osborne et al., 1989). Assuming the rate constant for spermine binding at 100 mV is diffusion limited and as high as esti-

mated for quaternary ammoniums (10^8–10^9 M^{-1} s^{-1}; Guo and Lu, 2001), the predicted current reduction caused by 1 nM spermine is 1–10% at the end of a 100-ms voltage pulse to 100 mV (full steady-state inhibition would require many seconds). Consequently, to limit the extent of channel block by spermine to at most a few percent during a 100-ms pulse, spermine concentration may need to be reduced to ≤1 nM. Even if the precise values of K$_d$ and k$_{on}$ (at 100 mV) for spermine are unknown, the above exercise illustrates the practical challenge posed by the need to lower spermine concentration to a level that will leave channel currents essentially unaffected. Not surprisingly, in cases where endogenous blockers cannot be adequately removed despite exhaustive perfusion, significant voltage-dependent channel inhibition persists (Fig. 11).

The problem of residual high-affinity inhibitors can be dramatically relieved, or even practically eliminated, by lowering channel affinity for intracellular cations. For example, a linear I-V curve is readily obtained in IRK1 channels containing the D172N mutation (Figs. 9 and 10; Guo and Lu, 2000a), which significantly lowers their affinity for intracellular spermine (e.g., Yang et al., 1995). Also as expected, we obtained satisfactory removal of endogenous blockers only with very small patches (Fig. 11). As stated in MATERIALS AND METHODS, to more effectively perfuse the patch we positioned the tip of the patch pipette in a rapid stream of the intracellular solution instead of perfusing the entire recording chamber. We also kept oocytes away from the recorded patch, since they are known to release substantial amounts of polyamines (Ficker et al., 1994; Lopatin et al., 1994).

Relaxation of inward IRK1 current induced by hyperpolarization has also been observed. Choe et al. (1999) found, and we confirmed here (Fig. 12), that some inward current relaxation results from channel block by divalent cations in the extracellular solution. Furthermore, Shieh (2000) showed that, in the absence of extracellular divalent cations but with HEPES present, lowering K$^+$ concentration reveals profound current relaxation after strong membrane hyperpolarization. Based on this finding, the author suggested that the current relaxation resembles C-type inactivation of voltage-activated *Shaker* K$^+$ channels, which is similarly "protected" by K$^+$. However, we found that this K$^+$-sensitive inward current relaxation can be also accounted for by residual HEP in the HEPES used to buffer extracellular pH (Figs. 13 and 14). On the basis of these findings, we argue that the K$^+$-sensitive current relaxation is also not an intrinsic gating property of these channels. The dramatic channel block induced by lowering K$^+$ on both sides of the membrane probably results from both a reduced competition of extracellular K$^+$ with extracellular blocking ions and a reduced

"knock off" effect of the blocking ions by intracellular K^{+} (Armstrong and Binstock, 1965; Armstrong, 1971; Yellen, 1984; MacKinnon and Miller, 1988; Neyton and Miller, 1988a,b; Spassova and Lu, 1998).

In summary, at the macroscopic level IRK1 channels inherently have practically ohmic characteristics although in principle, the I-V curve may exhibit slight outward rectification in the complete absence of any endogenous or exogenous blockers. In intact cells, the observed inward rectification of the I-V curve results from voltage-dependent block by intracellular cations such as Mg^{2+} and polyamines (Matsuda et al., 1987; Vandenberg, 1987; Ficker et al., 1994; Lopatin et al., 1994; Fakler et al., 1995). However, in excised membrane patches, perfused with solutions nominally devoid of Mg^{2+} and polyamines, the relaxation of both inward and outward IRK1 currents induced by voltage jumps and the resulting nonlinearity of the I-V curve is a reflection, not of intrinsic gating properties of IRK1 channels, but of the unusually high affinity of IRK1 for cations. Because of the extraordinarily high affinity for cations, traces of—usually insignificant—contaminants in commonly used organic pH buffers and metal ion chelators become highly significant and problematic in the study of IRK1 channels. Despite this, practically uninhibited (inward and outward) IRK1 currents and therefore linear I-V curves can be obtained, provided that the recorded membrane patch is adequately perfused and that both intracellular and extracellular solutions contain 100 mM KCl, 5 mM EDTA, and 10 mM phosphate at pH 7.6 or above.

REFERENCES

Aleksandrov, A., B. Velimirovic, and D.E. Clapham. 1996. Inward rectification of the IRK1 K^{+} channel reconstituted in lipid bilayers. *Biophys. J.* 70:2680–2687.

Armstrong, C.M. 1971. Interaction of tetraethylammonium ion derivatives with potassium channels of giant axons. *J. Gen. Physiol.* 58:413–437.

Armstrong, C.M., and L. Binstock. 1965. Anomalous rectification in the squid giant axon injected with tetraethylammonium. *J. Gen. Physiol.* 48:859–872.

Choe, H., H. Sackin, and L.G. Palmer. 1998. Permeation and gating of an inwardly rectifying potassium channel: evidence for a variable energy well. *J. Gen. Physiol.* 112:433–446.

Choe, H., L.G. Palmer, H. Sackin. 1999. Structural determinants of gating in inward-rectifier K^{+} channels. *Biophys. J.* 78:1988–2003.

Fakler, B., U. Brandle, E. Glowatzki, S. Weidemann, H.P. Zenner, and J.P. Ruppersburg. 1995. Strong voltage-dependent inward rectification of inward-rectifier K^{+} channels is caused by intracellular spermine. *Cell.* 80:149–154.

Fakler, B., J.H. Schultz, J. Yang, U. Schulte, U. Brändle, H.P. Zenner, L.Y. Jan, and J.P. Ruppersberg. 1996. Identification of a titratable lysine residue that determines sensitivity of kidney potassium channels (ROMK) to intracellular pH. *EMBO J.* 16:4093–4099.

Ficker, E., M. Taglialatela, B.A. Wible, C.M. Henley, and A.M. Brown. 1994. Spermine and spermidine as gating molecules for inward rectifier K^{+} channels. *Science.* 266:1068–1072.

Good, N.E., G.D. Winget, W. Winter, T.N. Connolly, S. Izawa, and R.M.M. Singh. 1966. Hydrogen ion buffers for biological research. *Biochemistry.* 5:467–477.

Guo, D., and Z. Lu. 2000a. Pore block versus intrinsic gating in the mechanism of inward rectification in strongly rectifying IRK1 channels. *J. Gen. Physiol.* 116:561–568.

Guo, D., and Z. Lu. 2000b. Mechanism of IRK1 channel block by intracellular polyamines. *J. Gen. Physiol.* 115:799–813.

Guo, D., and Z. Lu. 2001. Kinetics of inward-rectifier K^{+} channel block by quaternary ammonium ions: Dimension and properties of the inner pore. *J. Gen. Physiol.* 117:395–405.

Hoshi, T., W.N. Zagotta, and R.W. Aldrich. 1991. Two types of inactivation in *shaker* K^{+} channels: effects of alterations in the carboxy-terminal region. *Neuron.* 7:547–556.

Ishihara, K., A. Mitsuiye, A. Noma, and M. Takano. 1989. The Mg^{2+} block and intrinsic gating underlying inward rectification of the K^{+} current in guinea-pig cardiac myocytes. *J. Physiol.* 419:287–320.

Katz, B. 1949. Les constantes electriques de la membrane du muscle. *Arch. Sci. Physiol.* 2:285–299.

Kubo, Y., T.J. Baldwin, Y.N. Jan, and L.Y. Jan. 1993. Primary structure and functional expression of a mouse inward rectifier potassium channel. *Nature.* 362:127–133.

Lee, J.-K., J.A. Scott, and J.N. Weiss. 1999. Novel gating mechanism of polyamine block in the strong inward rectifier K channel Kir2.1. *J. Gen. Physiol.* 113:555–565.

Lopez-Barneo, J., T. Hoshi, S.H. Heinemann, and R.W. Aldrich. 1993. Effects of external cations and mutations in the pore region on C-type inactivation of *Shaker* potassium channels. *Receptors Channels.* 1:61–71.

Lopatin, A.N., E.N. Makhina, and C.G. Nichols. 1994. Potassium channel block by cytoplasmic polyamines as the mechanism of intrinsic rectification. *Nature.* 372:366–369.

Lu, T., A.T. Ting, J. Mainland, L.Y. Jan, P.G. Schultz, and J. Yang. 2001. Probing ion permeation and gating in a K^{+} channel with backbone mutations in the selectivity filter. *Nat. Neurosci.* 4:239–246.

Lu, Z., and R. MacKinnon. 1994. Electrostatic tuning of Mg^{2+} affinity in an inward-rectifier K^{+} channel. *Nature.* 371:243–246.

MacKinnon, R., and C. Miller. 1988. Mechanism of charybdotoxin block of the high-conductance, Ca^{2+}-activated K^{+} channel. *J. Gen. Physiol.* 91:335–349.

Matsuda, H. 1993. Effects of internal and external K^{+} ions on magnesium block of inwardly rectifying K^{+} channels in guinea-pig heart cells. *J. Physiol.* 435:83–99.

Matsuda, H., and J.D.S. Cruz. 1993. Voltage-dependent block by internal Ca^{2+} ions of inwardly rectifying K^{+} channels in guinea-pig ventricular cells. *J. Physiol.* 470:295–311.

Matsuda, H., A. Saigusa, and H. Irisawa. 1987. Ohmic conductance through the inward-rectifier K^{+} channel and blocking by internal Mg^{2+}. *Nature.* 325:156–159.

Neyton, J., and C. Miller. 1988a. Potassium blocks barium permeation through the high-conductance Ca^{2+}-activated K^{+} channel. *J. Gen. Physiol.* 92:549–567.

Neyton, J., and C. Miller. 1988b. Discrete Ba^{2+} block as a probe of

ion occupancy and pore structure in the high-conductance Ca^{2+}-activated K^+ channel. *J. Gen. Physiol.* 92:569–586.

Noble, D. 1965. Electrical properties of cardiac muscle attributable to inward going (anomalous) rectification. *J. Cell. Comp. Physiol.* 66:127–136.

Oishi, K., K. Omori, H. Ohyama, K. Shingu, and H. Matsuda. 1998. Neutralization of aspartate residues in the murine inwardly rectifying K^+ channel IRK1 affects the substate behavior in Mg^{2+} block. *J. Physiol.* 510:675–683.

Osborne, H.B., O. Mulner-Lorillon, J. Marot, and R. Belle. 1989. Polyamine levels during Xenopus laevis oogenesis: a role in oocyte competence to meiotic resumption. *Biochem. Biophys. Res. Commun.* 158:520–526.

Shieh, R.C. 2000. Mechanisms for the time-dependent decay of inward currents through cloned Kir2.1 channels expressed in *Xenopus* oocytes. *J. Physiol.* 526:241–252.

Shieh, R.C., S.A. John, J.-K. Lee, and J.N. Weiss. 1996. Inward rectification of IRK1 expressed in *Xenopus* oocytes: effects of intracellular pH reveal an intrinsic gating mechanism. *J. Physiol.* 494: 363–376.

Silver, M.R., and T.E. DeCoursey. 1990. Intrinsic gating of inward rectifier in bovine pulmonary artery endothelial cells in the presence and absence of internal Mg^{2+}. *J. Gen. Physiol.* 96:109–133.

Spassova, M., and Z. Lu. 1998. Coupled ion movement underlies rectification in an inward-rectifier K^+ channel. *J. Gen. Physiol.* 112:211–221.

Stanfield, P.R., N.W. Davies, P.A. Shelton, I.A. Khan, W.J. Brammer, N.B. Standen, and E.C. Conley. 1994. The intrinsic gating of inward rectifier K^+ channels expressed from the murine IRK1 gene depends on voltage, K^+ and Mg^{2+}. *J. Physiol.* 475:1–7.

Vandenberg, C.A. 1987. Inward rectification of a potassium channel in cardiac ventricular cells depends on internal magnesium ions. *Proc. Natl. Acad. Sci. USA.* 84:2560–2564.

Woodhull, A.M. 1973. Ionic blockage of sodium channels in nerve. *J. Gen. Physiol.* 61:687–708.

Xu, H., Z. Yang, N. Cui, L.G. Giwa, L. Abdulkadir, M. Patel, P. Sharma, G. Shan, W. Shen, and C. Jiang. 2000. Molecular determinants for the distinct pH sensitivity of Kir1.1 and Kir4.2 channels. *Am. J. Cell Physiol.* 279:C1464–C1471.

Yang, J., Y.N. Jan, and L.Y. Jan. 1995. Control of rectification and permeation by residues in two distinct domains in an inward rectifier K^+ channel. *Neuron.* 14:1047–1054.

Yellen, G. 1984. Relief of Na^+ block of Ca^{2+}-activated K^+ channels by external cations. *J. Gen. Physiol.* 84:187–199.

Yellen, G., D.C. Sodickson, and M.E. Jurman. 1994. An engineered cysteine in the external mouth of a K^+ channel allows inactivation to be modulated by metal binding. *Biophys. J.* 66:1068–1075.